Mechanics Research Communications 103 (2020) 103471

Contents lists available at ScienceDirect

Mechanics Research Communications

journal homepage: www.elsevier.com/locate/mechrescom

Three-point bending of an expanded-tapered sandwich beam—Analytical and numerical FEM study

Krzysztof Magnucki*, Jerzy Lewinski, Mariusz Far, Piotr Michalak

Łukasiewicz Research Network - Institute of Rail Vehicles "TABOR", Poznan, Poland

ARTICLE INFO

Article history:
Received 14 June 2019
Revised 12 September 2019
Accepted 27 December 2019
Available online 31 December 2019

Keywords:
Expanded-tapered sandwich beam
Three-point bending
Shear effec

ABSTRACT

The paper is devoted to expanded-tapered sandwich beam under three-point bending. The analytical model of the beam based on the broken-line hypothesis (zig-zag theory) is developed. The maximum deflection of the beam with consideration of the shear effect is analytically determined. Moreover, a numerical FEM model (SolidWorks) of the beam is formulated. The maximum deflections of example beams with the use of two methods are calculated and compared. The results are specified in Tables.

1. Introduction

1.1. Review of the literature

The sandwich structures initiated in the 20th century are intensively developed to-day. Vinson [1] described the basics of modeling of the sandwich structures, taking into account the articles from the 20th century. Thomsen and Vinson [2] presented a new high-order theory enabling consideration of sandwich beams and plates of varying thickness of the core. The core is rigid only in the out-of-plane direction, remaining flexible in the transverse direction. The proposed theory was verified by comparison of the numerical results to those obtained from finite element analysis, showing their good compliance. Icardi [3] developed a model enabling the analysis of laminated and sandwich beams, assuming a zig-zag approximation within each layer, with consideration of the transverse shear and the transverse normal stress. The results were compared to the 3-D elasticity solutions and various models available in literature. It was shown that the zig-zag representation improves accuracy of the results. Auciello and Ercolano [4] analyzed dynamic behavior of the Timoshenko beams taking into account the shearing deformation and the rotating inertia. The authors used the iterative variational Rayleigh–Ritz method for this purpose. The procedure was applied to tapered beams as an alternative to the usual FEM approach reported in the literature. Accuracy of the results obtained this way was very good. Maalek [5] dealt with the shear deflection of a tapering cantilever of rectangular cross section using the Timoshenko's beam theory. The formulae for the deflection have been derived in two ways, i.e. by integration of the Timoshenko's beam equation and with the method of virtual work. Good agreement with the finite element method and experimental results indicated effectiveness of the methods. Dado and Al-Sadder [6] studied very large deflections of prismatic and non-prismatic cantilevers subjected to various loads. The angle of the beam rotation was determined by a polynomial. Several cases of the cantilever shapes and loads were satisfactorily compared to the finite element results. Attarnejad et al. [7] developed a method of static analysis of arbitrarily tapered Timoshenko beams, based on the basic displacement functions. This allowed to achieve exact interpolation of the displacement field along the elements, thus ensuring fast convergence of the procedure. Effectiveness of the approach was verified for several cases of the static and dynamic examples. Shahba et al. [8] investigated free vibration and stability of functionally graded tapered Timoshenko beams using a finite element approach. The authors formulated an element that enabled consideration of variation of the cross-section profile and mechanical properties. Numerical examples validated good efficiency of the method. Challamel [9] examined the buckling of higher-order shear beam-columns using the enriched continuum approach. The buckling problem of a third-order shear beam-column was analytically solved using the gradient elasticity Timoshenko theory. The author presented several gradient elasticity Timoshenko models, inclusive of the buckling solutions for various structures and microstructured beams. Wang [10] studied the characteristics of the deformations of a tapered cantilever caused by its self-weight. The author derived asymptotic formulae for large deformations. The results so obtained were compared to the ones obtained by numerical integration. The relationships between the cantilever

* Corresponding author.
E-mail address: krzysztof.magnucki@tabor.com.pl (K. Magnucki).

https://doi.org/10.1016/j.mechrescom.2019.103471
0093-6413/

deformation and the taper degree and the cross section shape were found. Rajasekaran [11] used the differential transformation method and differential quadrature element method to investigate the free bending vibration of rotating functionally graded Timoshenko tapered beams. Effectiveness of both these approaches was verified by comparison with previously published results. Magnucki et al. [12] investigated deflection of a bent five-layer sandwich beam, the mechanical properties of which vary in its thickness direction. An mathematical model of the beam considering the shear effect was developed. Based on the principle of stationary total potential energy the system of differential equations of equilibrium was derived, allowing for formulation of the deflection formula. The effect of the thickness and mechanical properties of the binding layer on the beam deflection was analyzed. Auricchio et al. [13] considered a non-prismatic beam the cross-section of which varies along the beam axis. A model of a 2D linear-elastic non-prismatic beam enabled to develop a finite element describing the problem. Numerical results indicated that the proposed beam model correctly predicts the displacement and stress distributions of the beam. Pradhan et al. [14] analyzed static and dynamic stability of a pinned-pinned tapered sandwich beam with viscoelastic core. The beam was supported on a variable Pasternak foundation and subjected to pulsating axial load and a steady, one-dimensional temperature gradient. The Hamilton's principle allowed to formulate a set of equations solved afterwards with the general Galerkin's method. The principal regions of instability were investigated in accordance with various external conditions. Ai and Weaver [15] developed a sandwich beam model with a view to determine the effects of geometric taper and variable stiffness of the core on the static response of the beam. The minimum total potential energy method together with the Ritz technique enabled to obtain an approximate solution. It was found that variation of the axial stiffness of the core significantly affected displacements and stresses of the beams. Magnucki et al. [16] dealt with a short beam with symmetrically varying mechanical properties. The principle of stationarity of total potential energy served as a basis for formulation of the differential equations of equilibrium, solved afterwards for the case of three-point bending. The results were compared to those obtained with finite element method. Smyczynski and Magnucka-Blandzi [17] presented a strength analysis of a simply supported three layer beam composed of two metal facings, the metal foam core and two binding layers between the faces and the core. Two different nonlinear hypotheses of the deformation of the beam cross section were formulated. The results obtained based on the principle of the stationary potential energy were verified experimentally and numerically with the use of the finite element method. Magnucki et al. [18] devoted their work to a seven layer beam including the main core, two inner sheets, two second cores and two outer sheets. The zig-zag hypothesis enabled to determine the displacement and strain fields based on the stationary total potential energy. The effect of the core foam types on the deflections and stresses of the beam was analyzed. The analytical solution was compared to numerical FEM results. Magnucki [19] presented a problem of simply supported sandwich beams and I-beams of symmetrical structure subjected to three-point bending and uniformly distributed load. The models of deformation of planar beam cross section were assumed according to classical "broken line" hypothesis and nonlinear "polynomial" hypothesis. The system of the equations derived based on the principle of stationary total potential energy was solved for both load types. The deflections of the beams were calculated taking into account the shear effect. Magnucki et al. [20] delivered a comparative analysis of the stress state in bending of a homogenous tapered cantilever beam of rectangular cross section, calculated analytically and numerically (FEM). The analytical model is described based on bibliography, while the numerical FEM model is developed with the use of the SolidWorks software.

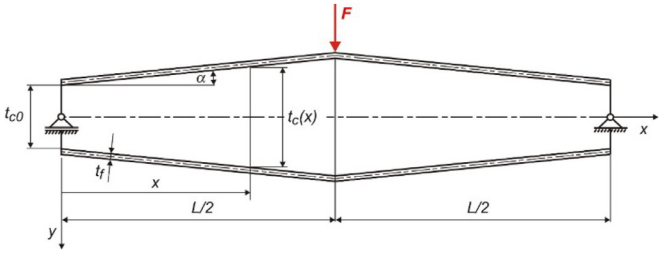

Fig. 1. Scheme of the expanded-tapered sandwich beam.

1.2. Description of the paper subject

The subject of the paper is an expanded-tapered sandwich beam of the length L and width b under three-point bending (Fig. 1).

The depth of the cross section of the beam

$$h(x) = 2\frac{t_f}{\cos\alpha} + t_c(x) \tag{1}$$

where: $t_c(x) = t_{c0} + 2x\tan\alpha$ - thickness of the core, t_{c0} - thickness of the core at the beam end, t_f - thickness of the faces, α - taper angle, x - coordinate ($0 \le x \le L/2$).

The thin-walled faces of the beam are made of metals of elastic constants E_f, ν_f, while the core is made of metal foam of elastic constants E_c, ν_c.

The main goal of the study consists in elaboration of an analytical model of the expanded-tapered sandwich beam under three-point bending based on the broken-line hypothesis (zig-zag theory). The approach to analytical modeling of the tapered beam enables to calculate the deflection and stress states. This analytical study of the expanded-tapered sandwich beam is an enhancement of the analytical study presented in [19] for the beams of constant depth. The essence of the enhancement consists in demonstration of significant difference between these two analytical models. The coefficients of the differential equations of equilibrium of the beams of constant depth are constant, while the coefficients of the differential equation of the expanded-tapered beams are the functions.

2. Analytical model of the beam – deflection

The deformation of a planar cross section of the beam determined with consideration of the broken-line hypothesis is shown in Fig. 2.

Therefore, the longitudinal displacements and strains for successive layers are as follows:

- the upper face $-h(x)/2 \le y \le -t_c(x)/2$

$$u(x,y) = -y\frac{dv}{dx} - u_1(x), \tag{2}$$

$$\varepsilon_x^{(u-f)}(x,y) = \frac{\partial u}{\partial x} = -y\frac{d^2v}{dx^2} - \frac{du_1}{dx},$$
$$\gamma_{xy}^{(u-f)}(x,y) = \frac{dv}{dx} + \frac{\partial u}{\partial y} = 0, \tag{3}$$

- the core $-t_c(x)/2 \le y \le t_c(x)/2$

$$u(x,y) = -y\left[\frac{dv}{dx} - 2\frac{u_1(x)}{t_c(x)}\right], \tag{4}$$

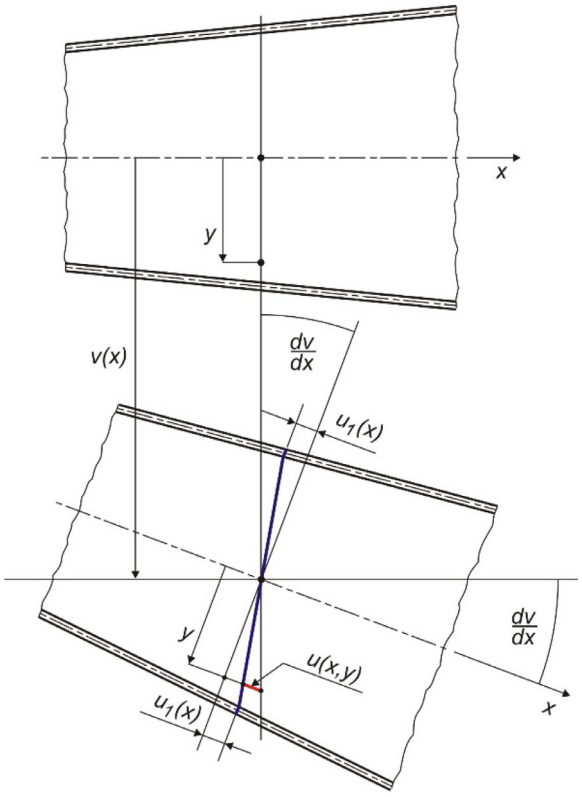

Fig. 2. Scheme of the deformation of a planar cross section of the beam.

$$\varepsilon_x^{(c)}(x,y)=\frac{\partial u}{\partial x}=-y\left[\frac{d^2v}{dx^2}-\frac{2}{t_c(x)}\frac{du_1}{dx}+4\frac{u_1(x)}{t_c^2(x)}\tan\alpha\right],$$
$$\gamma_{xy}^{(c)}(x,y)=\frac{dv}{dx}+\frac{\partial u}{\partial y}=\gamma_{xy}^{(c)}(x)=2\frac{u_1(x)}{t_c(x)}, \tag{5}$$

- the lower face $t_c(x)/2 \le y \le h(x)/2$

$$u(x,y)=-y\frac{dv}{dx}+u_1(x), \tag{6}$$

$$\varepsilon_x^{(l-f)}(x,y)=\frac{\partial u}{\partial x}=-y\frac{d^2v}{dx^2}+\frac{du_1}{dx},$$
$$\gamma_{xy}^{(l-f)}(x,y)=\frac{dv}{dx}+\frac{\partial u}{\partial y}=0, \tag{7}$$

The bending moment

$$M_b(x)=b\left\{\int_{-h(x)/2}^{-t_c(x)/2}y\sigma_x^{(u-f)}(x,y)dy+\int_{-t_c(x)/2}^{t_c(x)/2}y\sigma_x^{(c)}(x,y)dy+\int_{t_c(x)/2}^{h(x)/2}y\sigma_x^{(l-f)}(x,y)dy\right\}, \tag{8}$$

where the normal stresses

$$\sigma_x^{(u-f)}(x,y)=E_f\varepsilon_x^{(u-f)}(x,y),$$
$$\sigma_x^{(c)}(x,y)=E_c\varepsilon_x^{(c)}(x,y), \tag{9}$$
$$\sigma_x^{(l-f)}(x,y)=E_f\varepsilon_x^{(l-f)}(x,y).$$

It may be noticed that in accordance with the broken-line hypothesis the normal stresses are linear functions with respect to y-coordinate in the faces and the core.

After integration, with consideration of the longitudinal strains (3), (5), (7), one obtains the following differential equation

$$f_v(x)\frac{d^2v}{dx^2}-2f_u(x)\frac{du_1}{dx}+4e_ct_c(x)u_1(x)\tan\alpha=-12\frac{M_b}{E_fb}, \tag{10}$$

where: $e_c=E_c/E_f$ - dimensionless coefficient, and two functions

$$f_v(x)=2\frac{t_f}{\cos\alpha}\left[h^2(x)+h(x)t_c(x)+t_c^2(x)\right]+e_ct_c^3(x),$$
$$f_u(x)=6\frac{t_f}{\cos\alpha}\left[\frac{t_f}{\cos\alpha}+t_c(x)\right]+e_ct_c^2(x).$$

The shear force

$$V(x)=b\int_{-t_c(x)/2}^{t_c(x)/2}\tau_{xy}^{(c)}(x)dy=\frac{E_cb}{1+\nu_c}u_1(x), \tag{11}$$

where the shear stress

$$\tau_{xy}^{(c)}(x)=\frac{E_c}{2(1+\nu_c)}\gamma_{xy}^{(c)}(x). \tag{12}$$

It should be noticed that according to the broken-line hypothesis the shear stresses are equal to zero in the faces, while are constant in the core with respect to y-coordinate.

The differential Eq. (10) includes two unknown functions: $v(x)$ - the deflection, and $u_1(x)$ - the displacement (Fig. 2). The coefficients of this Eq. (10) are functions. The equation is solved for the generalized load. Taking into account [21] and [22], the generalized load is assumed in the following form:

- the intensity of the distributed load

$$q(\xi)=\tilde{q}(\xi)\frac{F}{L},$$
$$\tilde{q}(\xi)=\frac{k}{2\tanh(k/2)}\frac{1}{\cosh^2\left[k\left(\xi-\frac{1}{2}\right)\right]}, \tag{13}$$

where: k- dimensionless parameter ($0 \le k < \infty$), $\xi=x/L$ - dimensionless coordinate ($0 \le \xi \le 1$), and total load $F=L\int_0^1 q(\xi)d\xi$,

- the shear force

$$V(\xi)=\tilde{V}(\xi)F,$$
$$\tilde{V}(\xi)=-\frac{1}{2\tanh(k/2)}\tanh\left[k\left(\xi-\frac{1}{2}\right)\right]. \tag{14}$$

- the bending moment

$$M_b(\xi)=\tilde{M}_b(\xi)FL,$$
$$\tilde{M}_b(\xi)=\frac{1}{2k\tanh(k/2)}\ln\frac{\cosh(k/2)}{\cosh\left[k\left(\xi-\frac{1}{2}\right)\right]}. \tag{15}$$

The particular cases of the load:

- the uniformly distributed load ($k \to 0$)

$$\lim_{k\to0}q(\xi)=\frac{F}{L},\ \lim_{k\to0}V(\xi)=\frac{1}{2}(1-2\xi)F,$$
$$\lim_{k\to0}M_b(\xi)=\frac{1}{2}(1-\xi)\xi FL.$$

- the three-point bending ($k \to \infty$)

The example diagrams of the dimensionless intensity (13), shear force (14) and bending moment (15) for $k = 200$ are shown in Fig. 3.

It may be noticed that the generalized load for $k = 200$ approaches the three-point bending case. Therefore, the analytical study presented below is carried out for $k = 200$.

Based on comparison of the expressions (11) and (14), the displacement function in dimensionless coordinate takes the following form

$$u_1(\xi)=-\frac{1+\nu_c}{2\tanh(k/2)}\tanh\left[k\left(\xi-\frac{1}{2}\right)\right]\frac{F}{E_cb}. \tag{16}$$

Substituting the functions (15) and (16) into the Eq. (10), and after simple transformation, one obtains

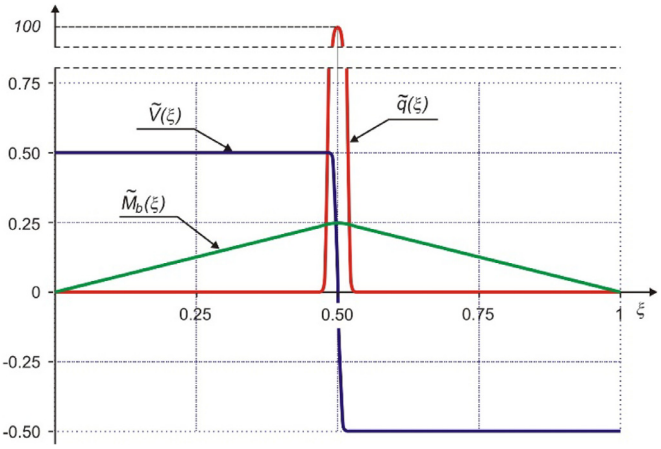

Fig. 3. Diagrams of generalized load for $k = 200$.

$$\frac{d^2v}{d\xi^2} = \left\{-(1+\nu_c)\left[\frac{k}{e_c\lambda}\varphi_1(\xi) - 2\varphi_2(\xi)\tan\alpha\right]\frac{1}{\lambda} - \frac{6}{k}\varphi_3(\xi)\right\}\frac{\lambda^3}{\tanh(k/2)}\frac{F}{E_f b}, \tag{17}$$

where dimensionless functions

$$\varphi_1(\xi) = \frac{\tilde{f}_u(\xi)}{\tilde{f}_v(\xi)}\frac{1}{\cosh^2[k(\xi-0.5)]},$$

$$\varphi_2(\xi) = \frac{\tilde{t}_c(\xi)}{\tilde{f}_v(\xi)}\tanh[k(\xi-0.5)],$$

$$\varphi_3(\xi) = \frac{1}{\tilde{f}_v(\xi)}\ln\frac{\cosh(k/2)}{\cosh[k(\xi-0.5)]},$$

$$\tilde{f}_v(\xi) = 2\frac{x_f}{\cos\alpha}\left[\tilde{h}^2(\xi) + \tilde{h}(\xi)\tilde{t}_c(\xi) + \tilde{t}_c^2(\xi)\right] + e_c\tilde{t}_c^3(\xi),$$

$$\tilde{f}_u(\xi) = 6\frac{x_f}{\cos\alpha}\left[\frac{x_f}{\cos\alpha} + \tilde{t}_c(\xi)\right] + e_c\tilde{t}_c^2(\xi),$$

$$\tilde{t}_c(\xi) = 1 + 2\xi\lambda\tan\alpha,$$

$$\tilde{h}(\xi) = 2\frac{x_f}{\cos\alpha} + \tilde{t}_c(\xi),$$

$x_f = t_f/t_{c0}$- dimensionless coefficient.

Integrating the Eq. (17) one obtains

$$\frac{dv}{d\xi} = \left\{C_1 - (1+\nu_c)\left[\frac{k}{e_c\lambda}\int\varphi_1(\xi)d\xi - 2\int\varphi_2(\xi)d\xi\tan\alpha\right]\frac{1}{\lambda} - \frac{6}{k}\int\varphi_3(\xi)d\xi\right\}\frac{\lambda^3}{\tanh(k/2)}\frac{F}{E_f b}. \tag{18}$$

The integration constant C_1 of this equation, based on the condition $dv/d\xi|_{1/2} = 0$, takes the following form

$$C_1 = (1+\nu_c)\left(\frac{k}{e_c\lambda}J_1 + 2J_2\tan\alpha\right)\frac{1}{\lambda} + \frac{6}{k}J_3, \tag{19}$$

where: $J_1 = \int_0^{1/2}\varphi_1(\xi)d\xi$,

$$J_2 = -\int_0^{1/2}\varphi_2(\xi)d\xi, J_3 = \int_0^{1/2}\varphi_3(\xi)d\xi.$$

Integrating the Eq. (18) one obtains the elastic deflection curve

Table 1
The results of analytical calculations of the beam of length $L = 320$ mm.

α [°]	0	1	2	3	4
$\tilde{v}_{\max}^{(Analyt)}$	6577.5	4109.2	2853.4	2117.1	1644.2
$v_{\max}^{(Analyt)}$[mm]	1.644	1.027	0.713	0.529	0.411

Table 2
The results of analytical calculations of the beams of length $L = 640$ mm.

α [°]	0	1	2	3	4
$\tilde{v}_{\max}^{(Analyt)}$	48,408.2	20,363.0	11,417.3	7363.4	5164.7
$v_{\max}^{(Analyt)}$[mm]	12.102	5.091	2.854	1.841	1.291

$$v(\xi) = \left\{C_2 + C_1\xi - (1+\nu_c)\left[\frac{k}{e_c\lambda}\int\int\varphi_1(\xi)d\xi^2 - 2\int\int\varphi_2(\xi)d\xi^2\tan\alpha\right]\frac{1}{\lambda} - \frac{6}{k}\int\int\varphi_3(\xi)d\xi^2\right\}\frac{\lambda^3}{\tanh(k/2)}\frac{F}{E_f b}, \tag{20}$$

where the integration constant $C_2 = 0$, based on the condition $v(0) = 0$.

Thus, the maximum deflection of the expanded-tapered sandwich beam for $\xi = 1/2$ is as follows

$$v_{\max}^{(Analyt)} = v\left(\frac{1}{2}\right) = \tilde{v}_{\max}^{(Analyt)}\frac{F}{E_f b}, \tag{21}$$

where the dimensionless maximum deflection

$$\tilde{v}_{\max}^{(Analyt)} = \left\{\frac{1}{2}C_1 - (1+\nu_c)\left[\frac{k}{e_c\lambda}J_{12} + 2J_{22}\tan\alpha\right]\frac{1}{\lambda} - \frac{6}{k}J_{32}\right\}\frac{\lambda^3}{\tanh(k/2)}, \tag{22}$$

where: $J_{12} = \int_0^{1/2}\int\varphi_1(\xi)d\xi^2$,

$$J_{22} = -\int_0^{1/2}\int\varphi_2(\xi)d\xi^2, J_{32} = \int_0^{1/2}\int\varphi_3(\xi)d\xi^2.$$

The detailed calculations are carried out for the exemplary expanded-tapered beams. The following data of the beams (Fig. 1) are adopted: thicknesses $t_{c0} = 14$ mm, $t_f = 1$ mm, the width $b = 20$ mm, taper angle $\alpha = 0^o, 1^o, ..., 5^o$, length $L = 320$ mm and $L = 640$ mm, load-force $F = 1$ kN, dimensionless parameter $k = 200$. The beam faces are made of steel of Young's modulus E_f=200 GPa, Poisson ratio $\nu_f = 0.3$, while the core is made of steel foam of Young's modulus E_c=3150 MPa and Poisson ratio $\nu_c = 0.05$ [17,18]. The detailed calculation results are specified in Tables 1 and 2.

3. Numerical FEM model of the beam - deflection

The FEM model of the expanded-tapered sandwich beam is developed with the use of the SolidWorks software package. Mechanical properties of the layers are equal to those used in analytical approach. Taking into account the symmetry of the beam the model may be confined to a quarter of the whole beam (Fig. 4), with appropriate boundary conditions imposed on it. The beam model is divided into 3D tetrahedral finite elements with 4 Jacobian points. The number of the nodes ranged from about $1.5\cdot10^6$ in case of $L = 320$ mm and α=0° to $7.1\cdot10^6$ for $L = 640$ mm and α=4°. The numbers of the elements amounted to $1.1\cdot10^6$ and $5.1\cdot10^6$, respectively.

Example of the mesh is shown in Fig. 5.

The beam is located in a Cartesian coordinate system the origin of which is placed in the beginning of the beam neutral axis (i.e. at the wall of the narrowed end). The longitudinal x axis is collinear

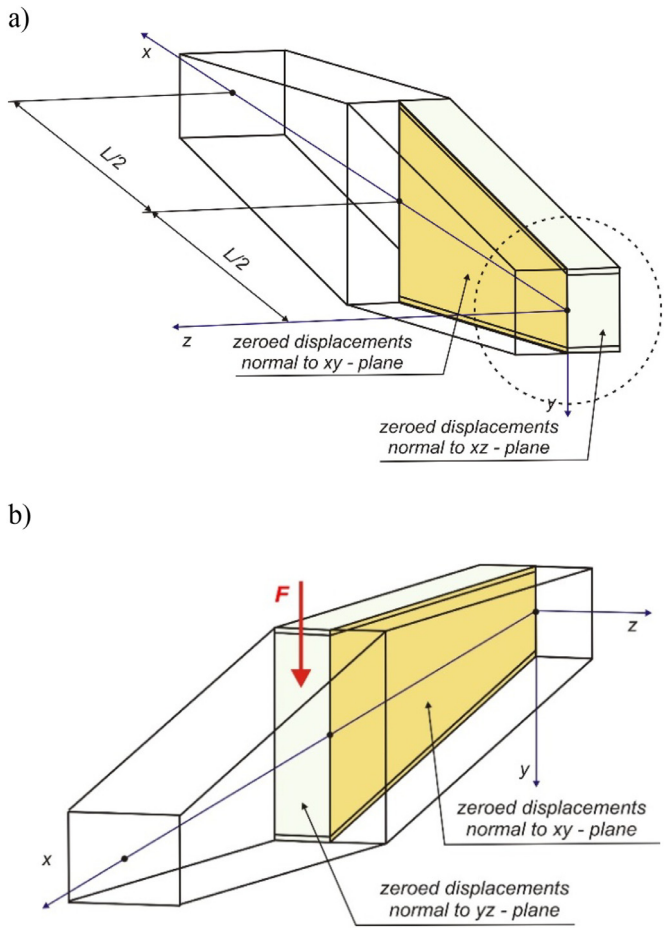

Fig. 4. Exemplary model of the expanded-tapered sandwich beam used for FEM computation.

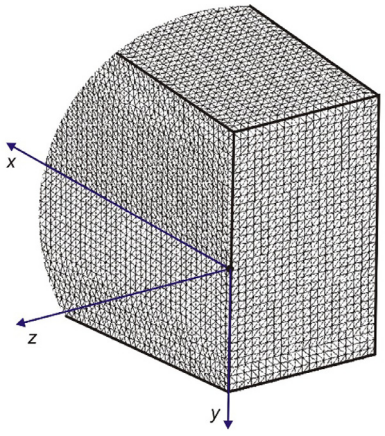

Fig. 5. A part of a FEM mesh (in the area marked in Fig. 4a with the dotted circle).

with the neutral axis, the y-axis is downward directed and z-axis is normal to the longitudinal middle plane of the beam.

The following boundary conditions imposed at the surfaces of the beam model ensure its proper behavior:

- The beam model is simply supported at its narrow edge (for $x = 0$), where the y displacements are zero.
- The x displacements are zero at the middle wall of the beam perpendicular to the neutral axis (for $x = L/2$). The wall is loaded with the force F parallel to the y-axis.

Table 3
The results of numerical - FEM calculations of the beams ($L = 320$ mm, $L = 640$ mm).

α [°]	0	1	2	3	4
$v^{(FEM)}_{\max,L=320}$ [mm]	1.634	1.006	0.691	0.509	0.394
$v^{(FEM)}_{\max,L=640}$ [mm]	12.024	5.040	2.814	1.810	1.268

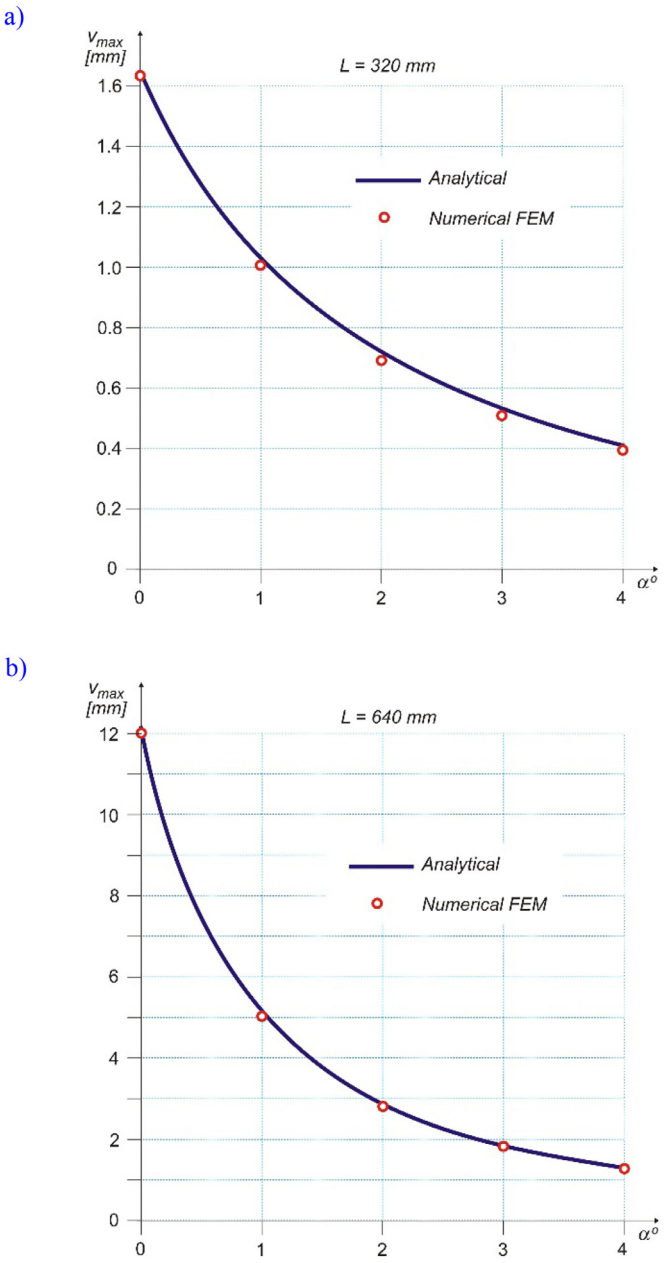

Fig. 6. Comparison of the deflection values calculated analytically and numerically: a) $L = 320$ mm, b) $L = 640$ mm.

- The z displacements are zero at the vertical longitudinal middle plane of the beam (for $z = 0$).

The SolidWorks calculations are carried out for the data adopted above for the analytical cases. The Table 3 presents maximum deflections calculated numerically.

The analytical and numerical results are graphically compared in Fig. 6.

Comparison of the numerical results with the values obtained analytically and shown in Tables 1 and 2 indicates very good con-

vergence of both series of the results. The differences do not exceed 4.3% in case of the shorter beam and 1.8% in case of the longer one.

4. Conclusion

The analytical model of the expanded-tapered sandwich beam developed with consideration of the "broken-line" hypothesis takes into account the shear effect.

The assumed generalized load enables to study bending of the beam for the load cases from a uniform to concentrated (three-point bending) one. The three-point bending is a particular case of this approach (Fig. 3). It should be noticed that the nearly concentrated load is applied to a certain surface rather ($k = 200$) than to a point. Therefore, the model achieves a practical meaning, since in actual structures the concentrated load must be applied through a membrane or rib, which distributes the load over a certain surface. The maximum deflection values (in the beam middle) are determined analytically with consideration of the shear effect for the exemplary beams.

An equivalent numerical FEM model was developed that enabled to make the calculations for the same beams. Such a model may be easily applied by the designers in practice.

Comparison of the results obtained analytically and numerically allows to find out that they comply each to other with good accuracy, with the differences not exceeding 4.3%.

Declaration of Competing Interests

The authors declare that they have no known competing financial interests or personal relationships that could have appeared to influence the work reported in this paper.

References

[1] J.R. Vinson, Sandwich structures, Appl. Mech. Rev. 54 (3) (2001) 201–214.
[2] O.T. Thomsen, J.R. Vinson, Modeling of tapered sandwich panels using a high-order sandwich theory formulation, AIAA J. 40 (9) (2002) 1867–1875.
[3] U. Icardi, Applications of Zig-Zag theories to sandwich beams, Mech. Adv. Mater. Struct. 10 (1) (2003) 77–97.
[4] N.M. Auciello, A. Ercolano, A general solution for dynamic response of axially loaded non-uniform Timoshenko beams, Int. J. Sol. Struct. 41 (18–19) (2004) 4861–4874.
[5] S. Maalek, Shear deflections of tapered Timoshenko beams, Int. J. Mech. Sci. 46 (5) (2004) 783–805.
[6] M. Dado, S. Al-Sadder, A new technique for large deflection analysis of non-prismatic cantilever beams, Mech. Res. Commun. 32 (6) (2005) 692–703.
[7] R. Attarnejad, A. Shahba, S.J. Semnani, Analysis of non-prismatic Timoshenko beams using basic displacement functions, Advan. Struct. Eng. 14 (2) (2011) 319–332.
[8] A. Shahba, R. Attarnejad, M.T. Marvi, S. Hajilar, Free vibration and stability analysis of axially functionally graded tapered Timoshenko beams with classical and non-classical boundary conditions, Compos. Part B: Eng. 42 (4) (2011) 801–808.
[9] N. Challamel, Higher-order shear beam theories and enriched continuum, Mech. Res. Commun. 38 (5) (2011) 388–392.
[10] C.Y. Wang, Large post-buckling of heavy tapered elastica cantilevers and its asymptotic analysis, Brief Note, Arch. Mech. 64 (2) (2012) 207–220.
[11] S. Rajasekaran, Free vibration of centrifugally stiffened axially functionally graded tapered Timoshenko beams using differential transformation and quadrature methods, Appl. Math. Mod. 37 (6) (2013) 4440–4463.
[12] K. Magnucki, M. Smyczynski, P. Jasion, Deflection and strength of a sandwich beam with thin binding layers between faces and a core, Arch. Mech. 65 (4) (2013) 301–311.
[13] F. Auricchio, G. Balduzzi, C. Lovadina, The dimensional reduction approach for 2D non-prismatic beam modelling: a solution based on Hellinger–Reissner principle, Int. J. Sol. Struct. 63 (2015) 264–276.
[14] M. Pradhan, M.K. Mishra, P.R. Dash, Stability analysis of an asymmetric tapered sandwich beam with thermal gradient, Proc. Eng. 144 (2016) 908–916.
[15] Q. Ai, P.M. Weaver, Simplified analytical model for tapered sandwich beams using variable stiffness materials, J. Sand. Struct. Mat. 19 (1) (2016) 3–25.
[16] K. Magnucki, M. Malinowski, E. Magnucka-Blandzi, J. Lewiński, Three-point bending of a short beam with varying mechanical properties, Compos. Struct. 179 (2017) 552–557.
[17] M.J. Smyczynski, E. Magnucka-Blandzi, The three-point bending of a sandwich beam with two binding layers – Comparison of two nonlinear hypotheses, Compos. Struct. 183 (2018) 96–102.
[18] K. Magnucki, S. Milecki, J. Lewinski, P. Kedzia, Bending of a seven layer beam with foam cores, Eng. Trans. 66 (3) (2018) 249–262.
[19] K. Magnucki, Bending of symmetrically sandwich beams and I-beams – Analytical study, Int. J. Mech. Sci. 150 (2019) 411–419.
[20] K. Magnucki, J. Lewinski, H. Stawecka, Stress state in the tapered beam bending – Analytical and numerical FEM studies, Rail Vehic. 2 (2019) 1–8.
[21] K. Magnucki, J. Lewinski, Bending of beams with symmetrically varying mechanical properties under generalized load – Shear effect, Eng. Trans. 67 (3) (2019) 441–457.
[22] K. Magnucki, J. Lewinski, R. Cichy, Bending of beams with bisymmetrical cross sections under non-uniformly distributed load – Analytical and numerical-FEM studies, Arch. Appl. Mech. 89 (2019) 2103–2114, doi:10.1007/s00419-019-01566-5.